

Appendix to DNA Reservoir Computing: A Novel Molecular Computing Approach

Alireza Goudarzi¹, Matthew R. Lakin¹, and Darko Stefanovic^{1,2}

¹ Department of Computer Science
University of New Mexico

² Center for Biomedical Engineering
University of New Mexico
alirezag@cs.unm.edu

Abstract. In this appendix, we justify the reduction of the nonlinear ODE system describing three coupled deoxyribozyme oscillators. We show that the kinetic simulation of the deoxyribozyme chemistry agrees with the result of the laboratory experiment. We make simplifying assumption that help us reduce a system of nine ODEs into three linear ODEs that is more amenable to mathematical analysis. We show that the reduced ODEs preserves the essentially properties of the original nonlinear ODEs and we use it to perform stability analysis on the system's dynamics.

A Kinetics and Oscillation in a Network of Deoxyribozyme Logic Gates

The fundamental units of our deoxyribozyme design are input, gate, substrate, and product. We denote the concentrations of these species by symbols $[I]$, $[G]$, $[S]$, $[P]$, where the subscript i is used as index to show compatible interacting reactants whenever we have more than one of each type of species in our reactions. The gate molecules become active in the presence of input molecules and cleave the substrate molecules [3]. As a result, substrate molecules turn into product molecules.

The reaction of gates and substrates and hence production of products can be described by $\frac{d[P]}{dt} = \beta[S][G]$, where $\beta = 5 \times 10^{-7} \text{ nM}^{-1} \text{ s}^{-1}$ is the reaction rate constant measured experimentally [1]. Figure 1a depicts the simulation of the actual experiment where 250 nM of gate molecules and 2500 nM of substrate molecules interact to produce products in the presence of different concentrations of input molecules (given in nM). For $[I] > [G]$, we observe that there is nonlinear growth in product concentration with a rate that is nearly independent of $[I]$. This simulation result agrees closely with the lab experiment reported in [1].

The effect of input molecules on gate molecules is very rapid, compared with the other reactions in the system. Since the only purpose of this reaction is to make the gates active we ignore this activation altogether and throughout this paper whenever we write $[G]$ we mean gate molecules that have been activated.

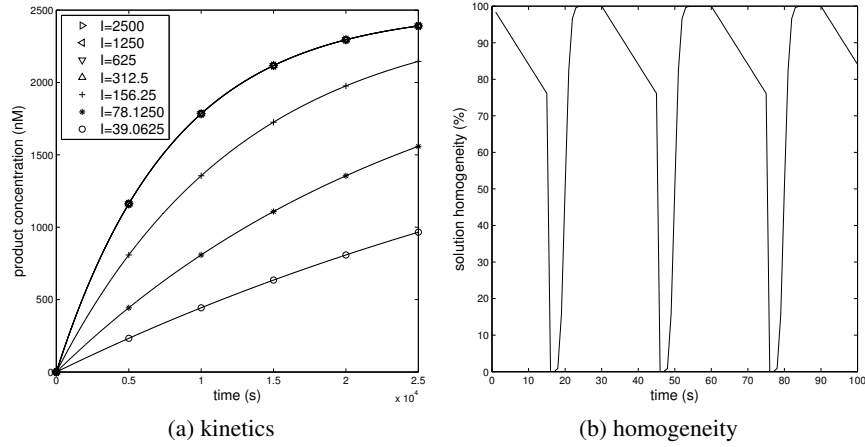


Fig. 1: Deoxyribozyme reaction rate and mixing behavior in a microfluidic reactor.(a) The simulated product concentration over time for different input concentrations (given in nM). The result agrees very well with the experimental results in [1]. (b)The calculated homogeneity of reactor content as the reactor goes through 15 s charging phase followed by a 15 s mixing phase [2].

Based on the results in [1], Farfel and Stefanovic [2] proposed an oscillator using three coupled deoxyribozyme NOT gates. In this design, one compatible pair of gate and substrate react and their products suppress the reaction of another pair of gate and substrate. For steady dynamics, there is an ongoing supply of new gates and substrates into the reactor, as well as an outflow of the reactor content to keep the volume constant. In the charging phase the new supplies come into the reaction chamber and old contents leave the chamber. Then influx and efflux stop and the mixing phase starts. During this phase the molecular species mix to create homogeneous solution. The reactions takes place as soon as the species are mixed. The charging and mixing phase repeat throughout the length of the simulation.

To describe the system, we need the influx of three different gate species and three corresponding substrate species denoted by $G_1^m, G_2^m, G_3^m, S_1^m, S_2^m, S_3^m$. Each species i of gates only binds to the substrate with matching index. We denote the corresponding concentration of interacting gates, substrates, and products in the reaction chamber by $[G_i], [S_i], [P_i]$. When explicitly talking about the concentrations at time t , we use $G_i(t), P_i(t)$, and $S_i(t)$. The total efflux rate, solution homogeneity, and chamber volume are given by constants E, H , and V . The system is then described by the following system of Ordinary Differential Equations (ODEs):

$$\begin{aligned}
\frac{d[G_1]}{dt} &= \frac{G_1^m(t) - E(t)[G_1]}{V} \\
\frac{d[G_2]}{dt} &= \frac{G_2^m(t) - E(t)[G_2]}{V} \\
\frac{d[G_3]}{dt} &= \frac{G_3^m(t) - E(t)[G_3]}{V} \\
\frac{d[P_1]}{dt} &= \beta H(t)[S_1] \max(0, [G_1] - [P_3]) - \frac{E(t)[P_1]}{V} \\
\frac{d[P_2]}{dt} &= \beta H(t)[S_2] \max(0, [G_2] - [P_1]) - \frac{E(t)[P_2]}{V} \\
\frac{d[P_3]}{dt} &= \beta H(t)[S_3] \max(0, [G_3] - [P_2]) - \frac{E(t)[P_3]}{V} \\
\frac{d[S_1]}{dt} &= \frac{S_1^m(t)}{V} - \beta H(t)[S_1] \max(0, [G_1] - [P_3]) - \frac{E(t)[S_1]}{V} \\
\frac{d[S_2]}{dt} &= \frac{S_2^m(t)}{V} - \beta H(t)[S_2] \max(0, [G_2] - [P_1]) - \frac{E(t)[S_2]}{V} \\
\frac{d[S_3]}{dt} &= \frac{S_3^m(t)}{V} - \beta H(t)[S_3] \max(0, [G_3] - [P_2]) - \frac{E(t)[S_3]}{V}
\end{aligned} \tag{1}$$

For the simulation of this system $E(t) = 0.12 \text{ nL s}^{-1}$, $G_i^m = 1.7940 \times 10^{-7} \text{ nmol s}^{-1}$, $S_i^m = 7.2921 \times 10^{-6} \text{ nmol s}^{-1}$, and $V = 7.54 \text{ nL}$. The reaction rate constant is the same for all the species and has the same value before. Homogeneity of the solution during the mixing phase $H(t)$ should be computed using the method in [2]. Figure 1b shows the calculated $H(t)$ during the simulation. However, this calculation is very expensive. It is possible to replace the result of the calculation by an average value of the calculated homogeneity $\bar{H}(t) = 0.7849$ as a constant. Note that because of the symmetry in the equations, for the oscillation to begin, we should break the symmetry in the initial value of the one of the species by giving it a different value. For our simulation we chose the following initial value $[P_1] = 1000 \text{ nM}$. The result of this simulation is shown in Figure 2 and matches the result reported in [2].

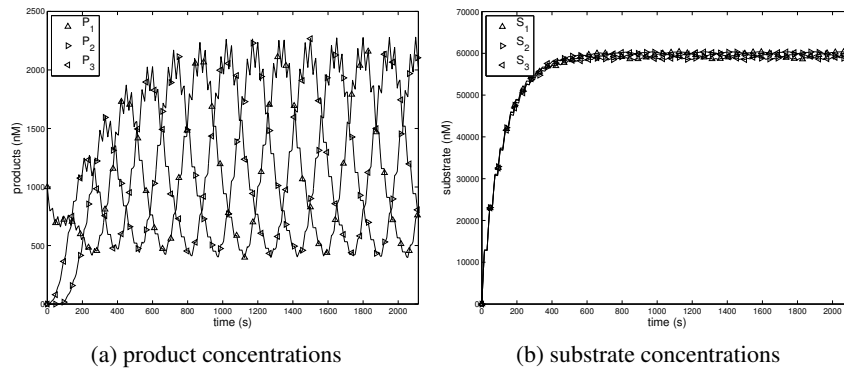


Fig. 2: The products and the substrates behavior in the reactor. (a) shows the oscillation in product concentrations in the reactor. (b) shows the substrate concentration in the reactor. The homogeneity is constant. These results match the original implementation in [2].

B Reduced Oscillator Model

In order to have better analytical grasp of the deoxyribozyme oscillator model discussed above, we can reduce the ODE system in Equation 1 into a form amenable to mathematical manipulation. Several of the details in the way simulation was previously done are related to the basic setup of the laboratory experiment initially conducted. First, the two phase charging and mixing operation was conceived because both gates and substrate flow into the microfluidic reaction chamber with a laminar flow. As a result the solution will not be well mixed and the reaction will not take place as expected. Therefore, separate charging and mixing phases were proposed in which a specific mixer that is designed to operate within the microfluidic reaction chamber mixes the solution within the chamber before different reactants can interact. However, in current setup gates are not consumed and their only role is to cleave the substrate into products. Therefore, we can assume a chamber in which gates are immobilized in the chamber. This eliminates the need for gate influx and separates the charging and mixing phases. In addition, we can adjust the gate and substrate concentration in a way that lets us safely remove the *max* function from Equation 1. This allows us to replace several of the variables with constants. We choose $h = \overline{H}(t)$, $g = [G_i]$. Moreover, because we eliminated the two-phase operation, the fluctuation in the substrate concentration (Figure 2b) now turns into a steady-state concentration which gives us a new constant $s = [S]$. The list of all the new constants and rates to be used in the reduced model is given in Table 1.

V	7.54 nL
$E(t)$	$8.8750 \times 10^{-2} \text{ nL s}^{-1}$
β	$5 \times 10^{-7} \text{ nM s}^{-1}$
h	0.7849
$[S_1], [S_2], [S_3]$	$6 \times 10^4 \text{ nM}$
$[G_1], [G_2], [G_3]$	$2.5 \times 10^3 \text{ nM}$

Table 1: New constants and rates for the reduced model.

After grouping all the constants together our new reduced model turns into a first-order linear ODE system given by Equation 2. The new constants are given in List 2. Since all the c_i and the b_i values are equal because of the symmetry of our model, we can suppress the indices and write c and b instead.

$$\begin{aligned}
 \frac{d[P_1]}{dt} &= b - c[P_3] - e[P_1] \\
 \frac{d[P_2]}{dt} &= b - c[P_1] - e[P_2] \\
 \frac{d[P_3]}{dt} &= b - c[P_2] - e[P_3]
 \end{aligned}
 \tag{2}$$

The fixed-point of the products in Equation 2 can be easily calculated by setting $\frac{d[P_i]}{dt} = 0$ and solving for $[P_i]$ as given in Equation 3:

new constant	old variables	value
e	$\frac{E(t)}{V}$	$1.1770 \times 10^{-2} \approx 1.175 \times 10^{-2}$
c_1	$\beta h(t)[S_1]$	2.35×10^{-2}
c_2	$\beta h(t)[S_2]$	2.35×10^{-2}
c_3	$\beta h(t)[S_3]$	2.35×10^{-2}
b_1	$c_1[G_1]$	5.88675×10^1
b_2	$c_2[G_2]$	5.88675×10^1
b_3	$c_3[G_3]$	5.88675×10^1

Table 2: New grouped constants used in Equation 2. We calculated these using the values in Table 1.

$$\begin{aligned}
[P_1]^* &= \frac{c[P_3]^* - b}{-e} = 1670 \\
[P_2]^* &= \frac{e[P_3]^* - b}{-c} = 1670 \\
[P_3]^* &= \frac{-b(ec - c^2 - e^2)}{c^3 - e^3} = 1670
\end{aligned} \tag{3}$$

The Jacobian of this system is given by Equation 4:

$$\mathcal{J} = \begin{bmatrix} \frac{d[P_1]}{d[P_1]} & \frac{d[P_2]}{d[P_1]} & \frac{d[P_3]}{d[P_1]} \\ \frac{d[P_1]}{d[P_2]} & \frac{d[P_2]}{d[P_2]} & \frac{d[P_3]}{d[P_2]} \\ \frac{d[P_1]}{d[P_3]} & \frac{d[P_2]}{d[P_3]} & \frac{d[P_3]}{d[P_3]} \end{bmatrix} = \begin{bmatrix} -e & -c_2 & 0 \\ 0 & -e & -c_3 \\ -c_1 & 0 & -e \end{bmatrix} = \begin{bmatrix} -e & -c & 0 \\ 0 & -e & -c \\ -c & 0 & -e \end{bmatrix}, \tag{4}$$

where eigenvalues are:

$$\begin{aligned}
\lambda_1 &= \frac{c}{2} - e - \frac{(\sqrt{3}c)}{2}i, \\
\lambda_2 &= \frac{c}{2} - e + \frac{(\sqrt{3}c)}{2}i, \\
\lambda_3 &= -c - e.
\end{aligned} \tag{5}$$

Not all eigenvalues are zero or purely imaginary so the Poincare-Lyapunov theorem holds and the system near its fixed-points approximately behaves like the linearized system described by the Jacobian.

Existence of an imaginary part in λ_1 and λ_2 indicates oscillatory behavior of the system. For $\frac{c}{2} > e$, the oscillations grow and the system becomes chaotic whereas for $\frac{c}{2} < e$, the oscillations die out over time. For sustained oscillation, we need to set $\frac{c}{2} = e$ as is the case in our reduction (cf. Table 2). One can also predict the period of the oscillation as $T = \frac{2\pi}{\theta}$, where θ is the coefficient of the imaginary part of the eigenvalues. We can easily verify that this is in fact the correct period in the simulation of the original model if the same values of the concentration for the reduced model are used. Figure 3 shows that the dynamics of oscillation in the reduced model and the original model are essentially identical. This justifies using the mathematically tractable reduced model for further analysis which we do in the the body of this paper.

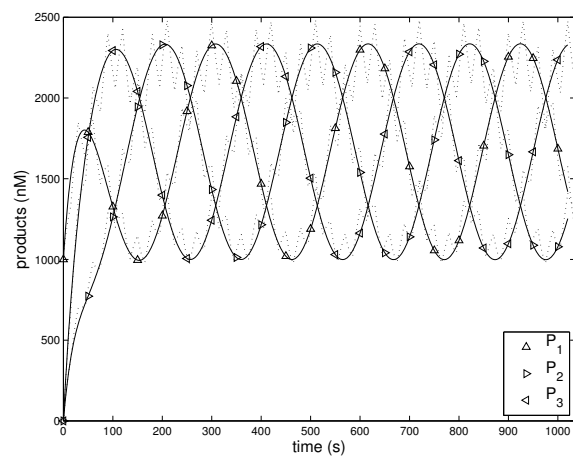


Fig. 3: Oscillation in the reduced model (solid line) versus the original model (dotted line). The efflux used for the reduced model is constant in time and given by $E(t) = 8.8750 \times 10^{-11}$, whereas the efflux used by the original model varies between the charging and the mixing phase and is given by $E(t) = 1.775 \times 10^{-10}$. The behaviors of the models match perfectly except for minor fluctuation due to the switching between charging and mixing in the original model. The reduced model preserves all essential aspects of the original model.

References

1. Morgan, C., Stefanovic, D., Moore, C., Stojanovic, M.N.: Building the components for a biomolecular computer. In Ferretti, C., Mauri, G., Zandron, C., eds.: DNA Computing. Volume 3384 of Lecture Notes in Computer Science. Springer Berlin Heidelberg (2005) 247–257
2. Farfel, J., Stefanovic, D.: Towards practical biomolecular computers using microfluidic deoxyribozyme logic gate networks. In Carbone, A., Pierce, N., eds.: DNA Computing. Volume 3892 of Lecture Notes in Computer Science. Springer Berlin Heidelberg (2006) 38–54
3. Stojanovic, M.N., Mitchell, T.E., Stefanovic, D.: Deoxyribozyme-based logic gates. Journal of the American Chemical Society **124**(14) (2002) 3555–3561